ISSN 1063-7737, Astronomy Letters, 2012, Vol. 38, No. 3, pp. 180–190. © Pleiades Publishing, Inc., 2012.
Original Russian Text © E.N. Sokov, I.A. Vereshchagina, Yu.N. Gnedin, A.V. Devyatkin, D.L. Gorshanov, V.Yu. Slesarenko, A.V. Ivanov, K.N. Naumov, S.V. Zinov'ev, A.S. Bekhteva, E.S. Romas, S.V. Karashevich, V.V. Kupriyanov, 2012, published in Pis'ma v Astronomicheskiĭ Zhurnal, 2012, Vol. 38, No. 3, pp. 208–218.

Observations of Extrasolar Planet Transits with the Automated Telescopes of the Pulkovo Astronomical Observatory

E. N. Sokov, I. A. Vereshchagina, Yu. N. Gnedin*, A. V. Devyatkin, D. L. Gorshanov, V. Yu. Slesarenko, A. V. Ivanov, K. N. Naumov, S. V. Zinov'ev, A. S. Bekhteva, E. S. Romas, S. V. Karashevich, and V. V. Kupriyanov

Pulkovo Astronomical Observatory, Russian Academy of Sciences, Pulkovskoe sh. 65, St. Petersburg, 196140 Russia

Received July 15, 2012

Abstract—Exoplanet observations have been performed on the automated Pulkovo Observatory telescopes. We have obtained 33 transit light curves for 16 known exoplanets and six transit observations for three exoplanet candidates discovered by the Kepler telescope. Based on our observations, we have reliably confirmed the existence of an exoplanet with an extremely large radius, $R_{\rm pl} = 1.83 \pm 0.16 R_{\rm Jup}$, in the system KOI 256 and detected a strong deviation of its orbital revolution from the theoretically predicted one. During the transit of the exoplanet WASP-12b across the stellar disk, we detected bursts that could be caused by the planet transit across spots on the star or by the presence of a satellite around this exoplanet. We detected possible periodic variations in the duration of the exoplanet transit across the stellar disk with time for HAT-P-12b that could be caused by variations in orbital inclination. The transit duration and depth, the central transit time, and the radius and orbital inclination of the planet have been estimated. The equilibrium temperature and albedo have been estimated for several exoplanets.

DOI: 10.1134/S106377371203005X

Keywords: *exoplanets, exoplanet candidates, transits.*

INTRODUCTION

Searching for and investigating planetary systems around other stars are among the central problems of modern astronomy. Such planets are commonly called exoplanets. In the coming decade, this research direction will become one of the leading ones. This is evidenced by the establishment of a new international institute to investigate exoplanets (extrasolar planets) within NASA (NASA Exoplanet Science Institute—NexSuI). An efficient program of exoplanet observations is currently being organized. The participation of 16 spaceborne observatories and 62 ground-based observatories, including the Keck interferometer (Danchi 2008), is planned in this program. Most of these observatories are already in operation. The first telescope specially launched to search for exoplanets, the Kepler Space Telescope (Borucki et al. 2011), already operates actively. By now, the Telescope has discovered 1235 exoplanet candidates, among which 18 have been confirmed.

The radial velocity method well known in astrophysics has long been the main method of searching for exoplanets. In this situation, it is based on the possibility of recording the apparent motion of the star itself around the center of mass of the star–planet system. The equations of celestial mechanics allow the following relation to be derived for such a system:

$$\frac{M_{\rm S}}{M_{\rm pl}} = \frac{a_{\rm pl}}{a_{\rm S}}, \qquad (1)$$

where $M_{\rm S}$ and $M_{\rm pl}$ and the masses of the star and the planet, respectively, $a_{\rm S}$ and $a_{\rm pl}$ are the semimajor axes of their orbits.

The expression for the angular size of the orbit around the center of mass of a binary system

$$\beta = \left[\frac{G}{4\pi^2}\right]^{1/3} \left[\frac{P}{M_{\rm S}}\right]^{2/3} \frac{M_{\rm pl}}{D}, \qquad (2)$$

where β is the angular size of the stellar orbit, G is the gravitational constant, P is the period of this system, and D is the distance from the observer to the star, follows from Newton's laws in the case where $M_{\rm S} \gg M_{\rm pl}$.

The radial velocity method allows only the projected orbital velocity, i.e., $V \sin i = V_r$, where V_r is the observed radial velocity and i is the orbital inclination to the line of sight, to be determined. The

*E-mail: gnedin@gao.spb.ru

spectroscopic observations that underlie this method require a very high accuracy.

A significant breakthrough in exoplanet research occurred after the discovery of the transit phenomenon. It consists in observing the drop in stellar brightness due to the planet transit across the disk of the central star. In this case, the depth of the drop in stellar brightness determines the ratio of the planetary radius to the stellar one

$$D = \left(\frac{R_{\rm pl}}{R_{\rm S}}\right)^2. \quad (3)$$

In general, Eq. (3) is valid if the stellar photosphere has a uniform distribution. In principle, the fact that the star also partially dims through limb darkening should be taken into account.

Systematic transit observations are necessary, because a series of systematic observations can experience variations due to the presence of other planets in the system or due to the existence of a Moon-type satellite around the main planet that provides the transit.

The method was called Transit Timing Variations (TTVs) and is successfully used in exoplanet observations (Miralda-Escude 2002; Agol et al. 2005; Narita 2009; Hoyer et al. 2011).

We performed transit observations for several known exoplanets. The most complete data on the results of the Kepler mission were published on February 2, 2011 (Borucki et al. 2011). For unconfirmed candidates presented in the latest catalog of all possible exoplanet candidates discovered by the Kepler Telescope, we have carried out transit observations for KO I 256b, KO I 425b, and KO I 194 for the first time and performed their subsequent analysis. Thus, we reliably confirmed the existence of an exoplanet around the star KO I 256 with an extremely large radius. The observations were performed with the ZA-320M Pulkovo Astronomical Observatory (PAO) telescope and the MTM-500M telescope at the Mountain Astronomical Station of the Pulkovo Observatory (MAS PAO) near Kislovodsk.

EXOPLANET OBSERVATIONS

We performed our observations of exoplanet transits on the automated PAO telescopes: the ZA-320M mirror astrograph and the MTM-500M Maksutov meniscus telescope. The ZA-320M Cassegrain mirror astrograph with a mirror diameter of 320 mm and a focal length of 3200 mm was installed on the PAO territory and has been operating since 1997. The telescope is equipped with a FLI IMG 1001E (1024 × 1024 pixels) CCD camera and has a $28' \times 28'$ field of view. The MTM-500M meniscus telescope was installed in 2007 at the Mountain Astronomical Station of the PAO at Mount Shadzhatmaz in the North Caucasus, near Kislovodsk. By its design, the telescope is a Maksutov meniscus system with an additional corrector. The mirror diameter is 500 mm, and the focal length is 4100 mm. The telescope is equipped with a SBIG STL 1001E (1024 × 1024 pixels) CCD camera and has $21' \times 21'$ field of view. Both telescope are equipped with B, V, R, and I filters corresponding to Johnson's international system (Straizys 1977) for photometric observations.

The ZA-320M and MTM-500M telescopes are automated on the same principle (Devyatkin et al. 2004; Kulish et al. 2009) and can be controlled remotely or operate according to a program that does not require the presence of an observer. The TelescopeControl program controls the operation of the coarse and fine pointing drives, the focusing devices, the filter replacement mechanisms, the dome positioning, etc. It also calculates the ephemerides of the observed objects at a specified time and controls the operation of the CCD camera via the CameraControl program. Devices based on digitized limbs and CCD cameras serve as the telescope rotation angle sensor (Kanaev et al. 2000; Devyatkin et al. 2008).

To process the photometric CCD observations, we used the APEX-II software package developed at the PAO (Devyatkin et al. 2009). The APEX-II package is completely automatic and has many options. The architecture and construction of the system are in many respects similar to those used in developing the IRAF, MIDAS, and IDL packages. Our package uses aperture photometry and PSF photometry (PSF fitting). APEX-II has a graphical shell that is needed for the cases where reference stars and an object should be chosen manually. This allows one to process short dense series of observations when the same reference stars are present on almost all frames. The referencing to specified photometric catalogs in this package is performed automatically.

When processing the photometric observations, for each series we chose, as a rule, 7–12 reference stars with a brightness close to that of the object located on the frame close to it to eliminate the atmospheric extinction effect. Based on the processing results, we studied the behavior of each reference star. If one of them was variable or if its behavior differed sharply from that of all the remaining stars, then it was excluded from the subsequent processing. The mean values of differences between the derived magnitudes of the reference stars and the magnitude of the object were the sought-for result—the object's light curve. The accuracy of the observations was determined using a check star that was chosen from the reference stars and was closest in brightness to the object. We performed the same procedure with the check star as that with the object—we found

Table 1. Results of our exoplanet observations on the ZA-320M and MTM-500M PAO telescopes

Object	Date	Transit duration, min	JD mid	Transit depth (m)	$R_{\rm pl}\,(R_{\rm Jup})$	i	Filter
HAT-P-12b	Mar. 19, 2011	143 ± 1.7	$2455630.51467 \pm 0.00049$	0.0298 ± 0.0008	1.124 ± 0.015	$88^{\circ}.94 \pm 0^{\circ}.4$	None
	Mar. 22, 2011	139.7*	$2455643.36874 \pm 0.00098$	0.0241 ± 0.0010	1.012 ± 0.02	88.67 ± 0.4	None
	Apr. 23, 2011	139.7*	$2455675.49546 \pm 0.00064$	0.0246 ± 0.0011	1.023 ± 0.022	88.64 ± 0.4	None
Qatar-1b	Mar. 2, 2011	92.7 ± 3.7	$2455623.49307 \pm 0.00095$	0.0250 ± 0.0019	1.212 ± 0.045	82.89 ± 0.38	None
	Mar. 15, 2011	102.9 ± 4.9	$2455636.27485 \pm 0.00116$	0.0269 ± 0.0014	1.257 ± 0.03	83.97 ± 0.38	None
	Apr. 18, 2011	96.5*	$2455670.35597 \pm 0.00092$	0.0277 ± 0.0016	1.275 ± 0.045	83.17 ± 0.38	None
WASP-12b	Oct. 12, 2010	180.0*	$2455482.52273 \pm 0.00169$	0.0168 ± 0.0017	1.934 ± 0.097	84.45 ± 3.0	None
	Feb. 18, 2011	180.0*	$2455611.30918 \pm 0.00132$	0.0155 ± 0.0011	1.858 ± 0.065	84.8 ± 3.0	None
	Feb. 19, 2011	171.3 ± 2.7	$2455612.39672 \pm 0.00083$	0.0161 ± 0.0007	1.894 ± 0.04	81.87 ± 3.0	None
	Mar. 26, 2011	175.1 ± 5.5	$2455647.32791 \pm 0.00173$	0.0189 ± 0.0017	2.051 ± 0.092	82.39 ± 3.0	None
WASP-14b	Mar. 11, 2011	163.2 ± 3.4	$2455632.57607 \pm 0.00105$	0.0097 ± 0.0005	1.194 ± 0.03	85.21 ± 0.67	R
	May 13, 2011	167.0*	2455695.40304 ± 0.0012	0.0118*	1.316*	85.42 ± 0.67	None
WASP-24b	May 10, 2011	155.5*	$2455692.43232 \pm 0.00286$	0.0075 ± 0.0023	0.929 ± 0.143	85.91 ± 0.65	None
ASP-40b	Feb. 18, 2011	98.6 ± 7.5	$2455614.60189 \pm 0.00173$	0.0167 ± 0.0023	1.085 ± 0.075	84.66 ± 0.55	None
	Apr. 26, 2011	109.0 ± 4.7	$2455678.42292 \pm 0.00102$	0.0189 ± 0.0011	1.154 ± 0.033	84.95 ± 0.55	None
WASP-10b	Aug. 3, 2010	127.8*	$2455412.48065 \pm 0.00073$	0.0397 ± 0.002	1.291 ± 0.032	87.01 ± 0.6	R
WASP-39b	Apr. 19, 2011	163.6 ± 3.9	$2455671.44314 \pm 0.00101$	0.0394 ± 0.002	1.843 ± 0.046	85.84 ± 0.23	None
TrES-3b	July 30, 2010	82.8 ± 2.8	$2455408.49819 \pm 0.00049$	0.0281 ± 0.0013	1.269 ± 0.029	82.12 ± 0.21	None
WASP-48b	May 8, 2011	191.5*	$2455690.37858 \pm 0.00239$	0.0110 ± 0.0013	1.715 ± 0.10	79.97 ± 0.61	None
GJ1214b	Apr. 11, 2011	52.8 ± 4.0	2455663.47904 ± 0.0011	0.0172 ± 0.0027	0.257 ± 0.02	88.30 ± 1.5	None
HAT-P-9b	Feb. 25, 2011	206.0*	2455618.285*	0.0107 ± 0.0011	1.276 ± 0.065	86.75 ± 0.2	None
HAT-P-20b	Feb. 28, 2011	102.6 ± 4.0	2455621.483*	0.0224 ± 0.003	0.963 ± 0.064	86.24 ± 0.2	None
HAT-P-18b	Apr. 10, 2011	162.9*	2455662.4*	0.0206 ± 0.021	1.002 ± 0.05	88.29 ± 0.3	None
	Apr. 21,-2011	162.9*	2455673.4308 ± 0.00509	0.0260 ± 0.0091	1.125 ± 0.2	88.15 ± 0.3	None
Kepler-6b	Oct. 5, 2010	240.5*	$2455475.27860 \pm 0.00455$	0.0148 ± 0.003	1.580 ± 0.16	90.00 ± 0.3	None
HD209458	Aug. 26, 2000	184.3*	2451783.298*	0.0150 ± 0.0031	1.310 ± 0.135	86.81 ± 0.06	R
	Sep. 2, 2000	184.3*	2451790.347*	0.0185 ± 0.0037	1.454 ± 0.145	86.62 ± 0.06	R
	Sep. 9, 2000	180.2 ± 9.9	$2451797.39721 \pm 0.00247$	0.0218 ± 0.0028	1.577 ± 0.1	86.21 ± 0.06	R
	Sep. 16, 2000	182.3 ± 9.3	2451804.446*	0.0161 ± 0.0021	1.357 ± 0.088	86.61 ± 0.06	R
	Oct. 18, 2000	184.3*	2451836.171*	0.0152 ± 0.0021	1.319 ± 0.09	86.80 ± 0.06	R
	Oct. 23, 2001	188.8 ± 7.1	$2452206.27266 \pm 0.00199$	0.0171 ± 0.0013	1.398 ± 0.053	87.03 ± 0.06	R
	Aug. 13, 2003	187.9 ± 5.8	$2452865.39544 \pm 0.00123$	0.0285 ± 0.0021	1.801 ± 0.065	86.43 ± 0.06	R
	Oct. 19, 2003	184.3*	2452932.367*	0.0178 ± 0.0021	1.427 ± 0.083	86.66 ± 0.06	R

* The default values that were taken from the catalog of data for exoplanets (http://exoplanet.eu/catalog-transit.php).

Table 2. Results of our observations of exoplanet candidates on the ZA-320M and MTM-500M PAO telescopes

Object	Date	Transit duration, min	JD mid	Transit depth	R_{pl} (R_{Jup})	i	Filter
KO I 256b	Mar. 3, 2011	51.6 ± 7.7	2455624.55597 ± 0.00199	0.0449 ± 0.0108	2.161 ± 0.255	73.°64 ± 1.°0	None
	Apr. 30, 2011	74.9 ± 6.4	2455682.47101 ± 0.00165	0.0425± 0.0084	2.104 ± 0.2	74.52 ± 1.0	None
	May 7, 2011	73.4*	2455689.36775 ± 0.00371	0.0167 ± 0.0073	1.327 ± 0.3	75.61 ± 1.0	None
	May 29, 2011	56.6 ± 2.7	2455711.40231 ± 0.00074	0.0264± 0.0027	1.664 ± 0.084	74.50 ± 1.0	None
KO I 425b	Apr. 18, 2011	92.2*	2455670.44525 ± 0.01431	0.0170 ± 0.0121	1.107 ± 0.4	86.05 ± 1.0	None
KO I 194b	Mar. 1, 2011	120.0*	2455621.58635 ± 0.00656	0.0294 ± 0.0152	1.308 ± 0.34	86.50 ± 1.0	None

* The values were not calculated but were taken from the catalog for exoplanet candidates (Borucki et al. 2011).

the mean difference between its brightness and the brightness of the remaining reference stars and calculated the standard deviation for the derived light curve, which was considered to be the accuracy of the observations. The best photometric accuracy was $0^m.003$ and $0^m.001$ for the ZA-320M and MTM-500M telescopes, respectively.

MAIN RESULTS OF EXOPLANET OBSERVATIONS

Over the period from August 2010 to June 2011, we obtained 31 photometric observations of the transits of exoplanets and exoplanet candidates on the ZA-320M and MTM-500M telescopes. Long before this period, from 2000 to 2007, we also performed photometric observations of the transits of the exoplanet HD 209458 on the ZA-320M telescope. Based on all observations, we constructed the light curves during the planet transit across the stellar disk.

Thus, the light curves were obtained for the already known exoplanets HAT-P-12b, Qatar-1b, WASP-12b, WASP-14b, WASP-40b, WASP-10b, WASP-39b, TrES-3b, WASP-48b, GJ1214b, Kepler-6b, HAT-P-18b, HAT-P-9b, HAT-P-20b, HD209458b as well as the exoplanet candidates KO I 425b, KO I 194b, KO I 256b.

The site of the Czech Astronomical Society provides a page (http://var2.astro.cz/ETD) on which the authors of the site collect the transit observations for all known transiting exoplanets and, since recent times, exoplanet candidates. In addition, a program was connected to this site that allows the transit to be modeled based on the observational data uploaded by a user. The model includes the physical parameters of the parent star, the parameters of the planet, and its orbital elements. The modeling results are the central transit time, the transit duration, the transit depth, the radius of the planet and its orbital inclination, the model light curve that fits best the corresponding observational data, and an estimate of the accuracy of these data (see Poddany et al. 2010).

We used this site to model the observed transits based on the derived light curves. The parameters obtained are presented in Table 1 for known exoplanets and in Table 2 for the exoplanet candidates KO I 425b, KO I 194b, KO I 256b.

Figure 1 presents examples of the derived transit light curves for the known exoplanets HAT-P-12b and WASP-14b, Fig. 2 shows plots for the confirmed exoplanet candidate KO I 256b, and Fig. 3 presents our observations for the exoplanet candidates KO I 194b and KO I 425b. All of the plots for which the model light curve was drawn and the linear trend was subtracted were taken from the Exoplanet Transit Database (ETD) for exoplanets and exoplanet candidates (http://var2.astro.cz/ETD/).

ANALYSIS OF OBSERVATIONAL DATA

The Exoplanet Candidates KO I 256b, KO I 425b, and KO I 194b

One of the main results of our observations is a confirmation of the transits for the exoplanet candidates KO I 256b, KO I 425b, and KO I 194b. Based on a series of four observations for the exoplanet candidate KO I 256b, we can say with confidence that a planet is present in this system. For each of KO I 425b and KO I 194b, we obtained one light curve, suggesting the probable presence of a planet in these

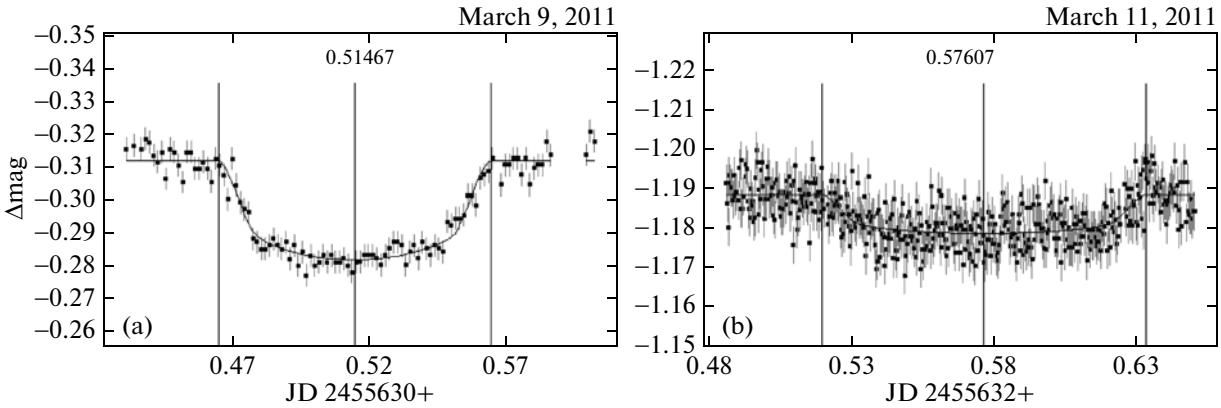

Fig. 1. Examples of the light-curve observations performed with the ZA-320M telescope during the exoplanet transit across the stellar disk with a subdivision into zones—before the beginning of the transit, from the beginning to the middle, from the middle to the end of the transit, and after the transit: (a) the transit of the exoplanet HAT-P-12b, (b) the transit of the exoplanet WASP-14b.

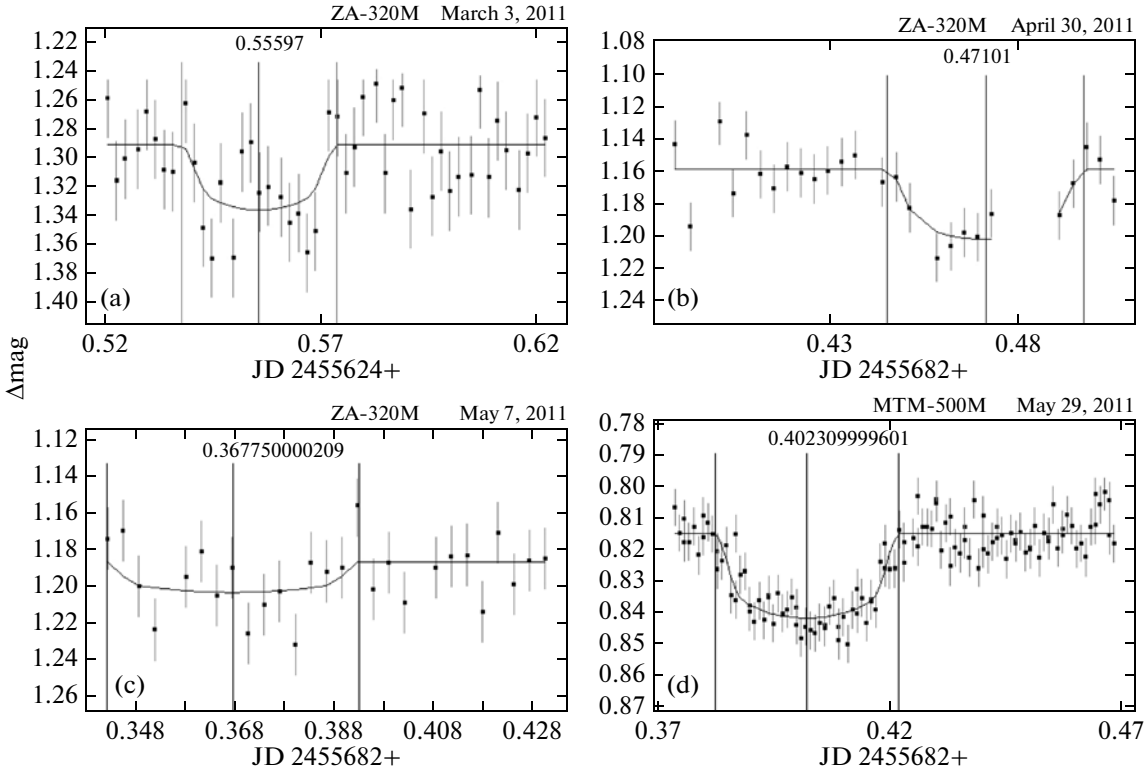

Fig. 2. Light curves during the transit of the exoplanet candidate KO I 256b on (a) March 3, 2011, (b) April 30, 2011, (c) May 7, 2011, and (d) May 29, 2011. The observations were performed with the ZA-320M and MTM-500M telescopes.

systems. However, their more reliable confirmation requires further observations both by the method of the planet transit across the stellar disk and by other methods.

Interesting results were obtained by analyzing the observations of the candidate KO I 256b (2MASS ID: 19004443 + 4933553, Kepler ID: 256.01, $M_V = 15.373$). The radius of the exoplanet KO I 256b was determined from the observations performed with the ZA-320M and MTM-500M telescopes as well as by Peter Lake with a 20″ reflector (see http://var2.astro.cz/EN/tresca/transit-detail.php?id

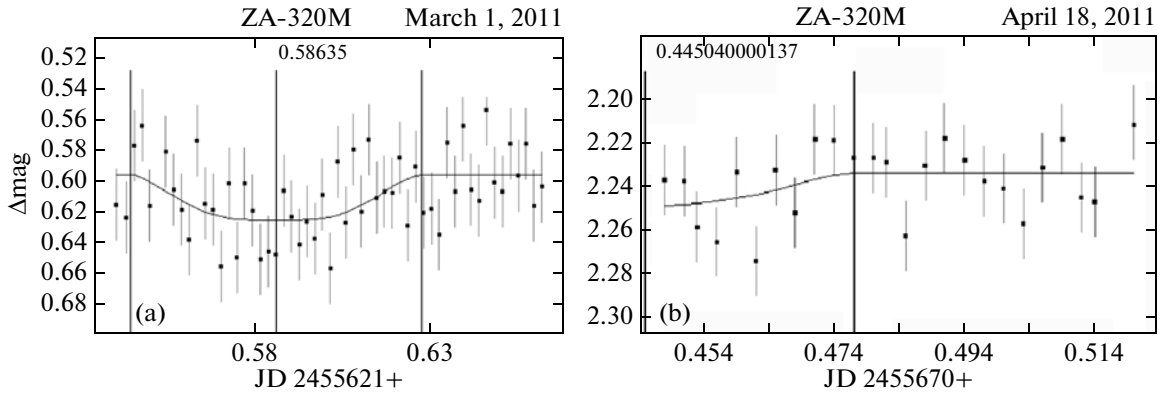

Fig. 3. Light curves during the transits of exoplanet candidates: (a) KOI 194b, (b) KOI 425b. The observations were performed with the ZA-320M telescope.

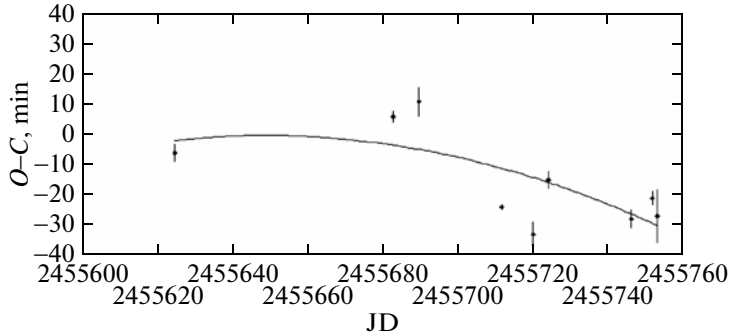

Fig. 4. $O-C$ diagram for nine observations of KOI 256b.

= 1307443185; http://.../id=1307795834; http://.../id=1309750254; http://.../id=1310292531) and Anthony Ayiomamitis with a 305-mm astrograph (see http://var2.astro.cz/EN/tresca/transit-detail.php?id=1310169870) with weights; it is $R_{\rm pl} = 1.83 \pm 0.16 R_{\rm Jup}$. Thus, KO I 256b can be attributed to hot Jupiters of an extremely large size.

The observations show a complex behavior of the $O-C$ residuals for the mid-transit time, the transit depth and duration, and the orbital inclination of the exoplanet to the plane of the sky. The $O-C$ residual reaches 33 min. Table 3 lists the $O-C$ residuals for our observations and the observations of other authors taken from the ETD (http://var2.astro.cz/ETD/). It should be noted that this residual is unstable (Fig. 4). This can be caused by the influence of nongravitational effects on the orbital motion of the planet around the star or by the presence of perturbing bodies in the system under consideration; other planets can act as the latter. The orbital inclination of this exoplanet with respect to the plane of the sky was estimated from the observations to be $74\overset{\circ}{.}77 \pm 0\overset{\circ}{.}36$, i.e., it differs greatly from 90°, so that the planet passes over the very edge of the stellar disk during its transit. Therefore, we may not see the transits of other planets if they lie roughly in the same plane as the planet under consideration, but at a greater distance from the star, but only feel their influence on the change in the period and orbital elements of the observed exoplanet.

The difference in transit durations for KO I 256b is also worth noting (Table 2). This difference may suggest that this planet has an orbital eccentricity. As a result of the planet's orbital eccentricity, the transit duration decreases significantly when the planet is at periastron and increases if the planet is at apastron. According to Tingley and Sackett (2005) (see Eq. (7) in their paper), the dimensionless quantity τ corresponding to the ratio of the transit duration in the presence of an orbital eccentricity to the transit duration in the case of a circular orbit is (see also Barnes 2007; Burke 2008)

$$\tau = \frac{\sqrt{1-e^2}}{1+e\cos\omega}\sqrt{1-\rho^2\left[\frac{1-e^2}{1+e\cos\omega}\right]^2\cos^2 i}, \quad (4)$$

Table 3. Deviations of the mid-transit times derived from the observed light curves of KOI 256b from the theoretical ones and the rms error σ of the observed mid-transit times

JD	$O-C$, min	σ	3σ	Telescopes
2455624.55597	−6	3	9	ZA-320M
2455682.47101	6	2	6	ZA-320M
2455689.36775	11	5	15	ZA-320M
2455711.40231	−24	1	3	MTM-500M
2455719.68100	−33	4	12	20″ Peter Lake reflector
2455723.81674	−15	3	9	20″ Peter Lake reflector
2455745.86664	−28	3	9	20″ Peter Lake reflector
2455751.38616	−21	2	4	Ayiomamitis 305-mm astrograph
2455752.76007	−27	9	27	20″ Peter Lake reflector

where $\rho = a/(R_s + R_{pl})$, R_s is the radius of the star, R_{pl} is the radius of the planet itself, a is the distance to the pericenter of the planetary orbit: $\omega = 0°$ and $\omega = 180°$ correspond to the pericenter and apocenter of the orbit, respectively. If $e = 0.6$, then $\tau = 0.5$ for the transit at perihelion and $\tau = 2$ for the transit at aphelion.

According to the data in Table 2, the orbit of KO I 0256b may be considered circular within 2σ. We will then derive the following constraints on the orbital radius:

$$r^2 \cos^2 i \ll 1, \quad a \ll R_s/\cos i; \quad R_s \gg R_{pl}. \quad (5)$$

For a stellar radius $R_s \approx 10^{11}$ cm, we obtain $a \ll 0.03$ AU. On the other hand, if we use the ratios of the observed maximum and minimum transit durations, $\tau \approx 1.45$, then we will obtain an orbital eccentricity $e \approx 0.2$.

Periodic Bursts on the Light Curve during WASP-12b Transits

We carried out four observations of the exoplanet WASP-12b on the ZA-320M telescope. During the February 18, 2011 and February 19, 2011 transits, bursts of an unknown nature are clearly seen on the light curves (Fig. 5) during the exoplanet transit across the stellar disk itself.

Such bursts were also detected on several light curves of other authors during the transit of the exoplanet WASP-12b in the ETD (http://var2.astro.cz/ETD/etd.php?STARNAME= WASP-12&PLANET= b). Figures 5 and 6 give examples of such plots and the residuals after the subtraction of all points of the observed light curve from the model one.

Based on all these plots, we estimated the possible periods of the bursts and their amplitudes by the Clean method (Vityazev 2001b) and using a wavelet analysis (Vityazev 2001a). We obtained the possible periods $P \approx 0^d.09$ and $P \approx 0^d.084$ well as the amplitude $A \approx 0^m.0015$ using both methods. Such similar data may be indicative of a possible repeatability of the same phenomenon during the revolution of the exoplanet around the star. Such phenomena can include: the physical activity of the star itself manifested as a periodic appearance of spots on it and the variation in the stellar disk area eclipsed during the transit, which can be caused either by the ellipsoidal shape of the exoplanet WASP-12b or by the existence of an exomoon revolving around the planet.

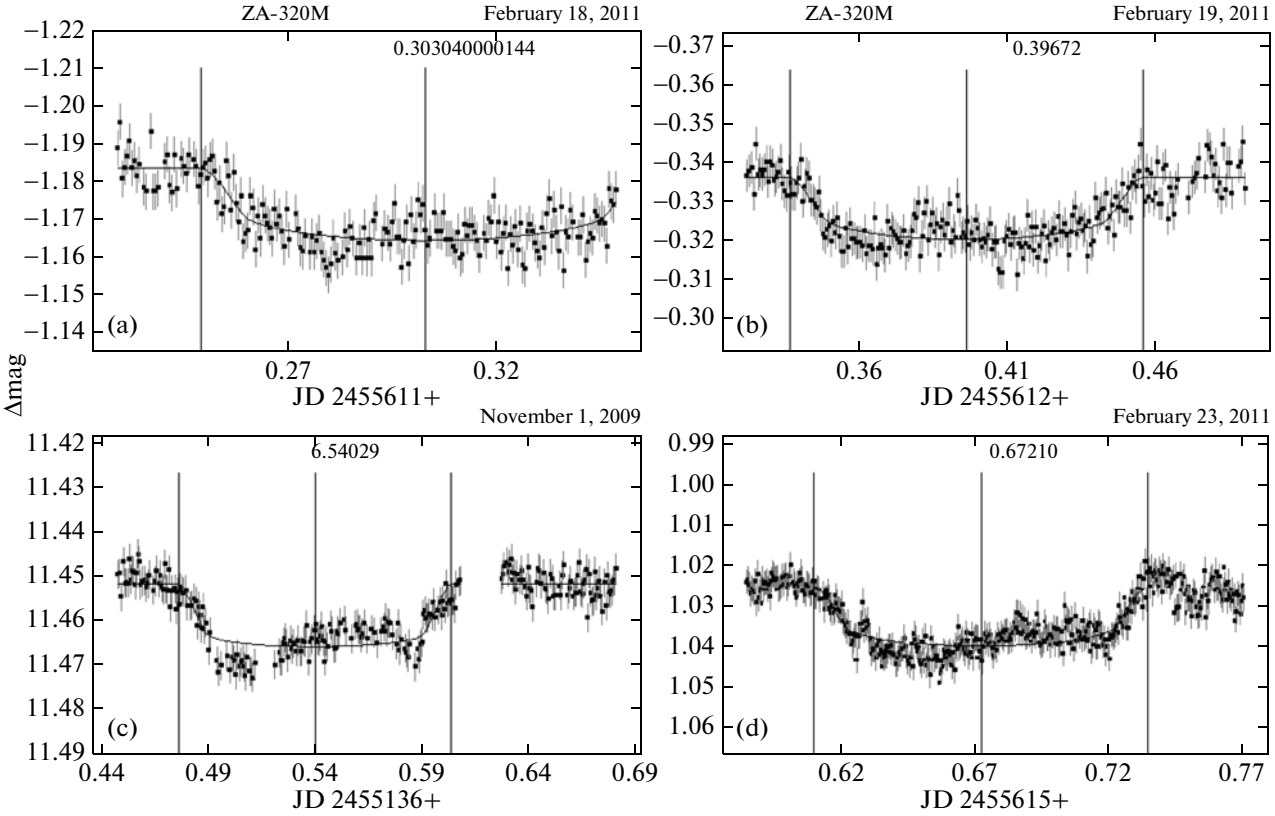

Fig. 5. Brightness variations with the manifestation of bursts during the February 18, 2011 (a) and February 19, 2011 (b) transits of the exoplanet WASP-12b; the observations were performed on the ZA-320M telescope. The observations performed by L. Kornos and P. Veres on November 1, 2009 (c) and by E. Rich and S. Irwin on February 23, 2011 (d) (the data were taken from the ETD http://var2.astro.cz/EN/tresca/transit-detail.php?id=1257173994; http://var2.astro.cz/EN/tresca/transit-detail.php?id=1300395529).

The ellipsoidal shape of this exoplanet could produce such bursts on the light curve during its transit. However, at such a close distance of the planet from the star (0.023 AU), the spin period of the exoplanet must be synchronized with its orbital period due to tidal interactions and, hence, its one side must always face the star. Spots on the stellar surface can also produce such brightness variations. However, the observed bursts are very similar in duration, profile, and amplitude, although about two years elapsed between the observations made by different authors. Thus, one of the probable causes of such busts is the existence of a satellite around this exoplanet. We can roughly estimate its size by assuming the amplitude of the brightness variations due to the presence of an exomoon to be $0^{\rm m}.0015$; it is $R \approx 6.4R_{\rm Earth} \approx 0.57R_{\rm Jup}$. It should be noted that the size of the exoplanet itself is $R = 1.736 \pm 0.092R_{\rm Jup}$ (Chan et al. 2011).

Further observations of the exoplanet WASP-12b are needed to check the validity of these assumptions and to understand the causes of such bursts in more detail.

Possible Variations in the Orbital Inclination of the Exoplanet HAT-P-12b

From the ETD (http://var2.astro.cz/ETD/), we chose the observations of the exoplanet HAT-P-12b with small errors in the observational data. Based on them, we analyzed the variations in the duration of exoplanet transits across the stellar disk and its orbital inclination to the plane of the sky. We found a slight change in these parameters over the total period of joint observations from May 2009 to June 2011. As we see from Fig. 7, the change in transit duration is 6 min. The change in the duration of the exoplanet transit across the stellar disk can be caused by a variation in the orbital inclination of the exoplanet. To test this assumption using the ETD data on the inclinations for each observation, we plotted the orbital inclination of HAT-P-12b against time (see Fig. 8). As can be clearly seen from this plot, the inclination follows the time profile of the transit duration. However, at present, the data are insufficient for a reliable confirmation and study of the variability of these parameters with time; further observations of

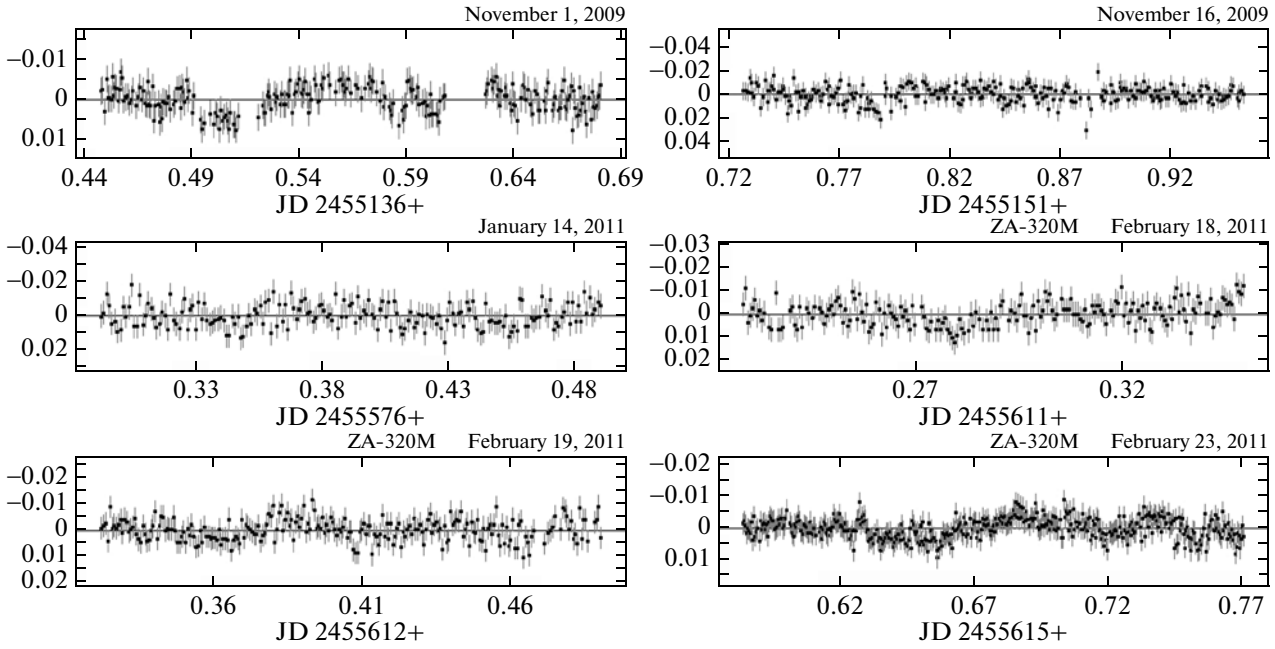

Fig. 6. Residuals from the subtraction of the model light curve from the observed ones in which bursts were noticed. The data were taken from the ETD (http://var2.astro.ca/ETD/).

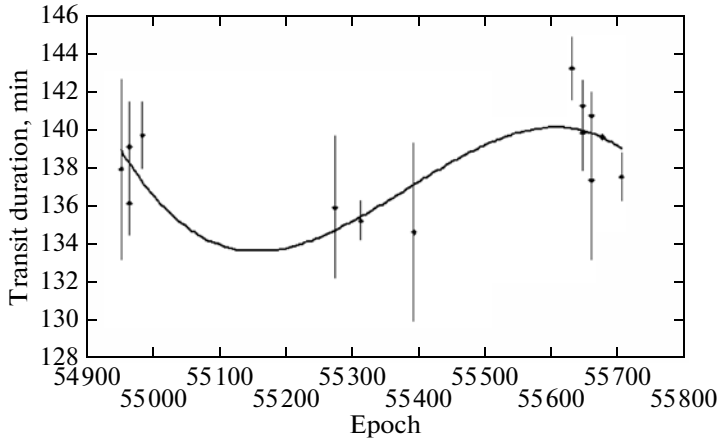

Fig. 7. Transit duration for HAT-P-12b versus time.

the exoplanet HAT-P-12b are needed. However, if this dependence will be confirmed by further observations, then we will be able to talk about the possible presence of perturbing bodies; the neighboring planets of this system can act as the latter.

Determining the Equilibrium Temperature and Geometrical Albedo of Exoplanets

Another important result that can be extracted by analyzing the results of our observations and other, already published results of exoplanet observations is the determination of the equilibrium temperature T_{eq} and, where possible, albedo A of the planet. The recently published paper by Demory et al. (2011) is the central publication that can provide a basis for such a work. These authors presented a detailed relationship between the equilibrium temperature and albedo of a planetary atmosphere obtained within Kurucz's model for the radiation of a stellar atmosphere and under the assumption about a blackbody temperature of the planetary atmosphere.

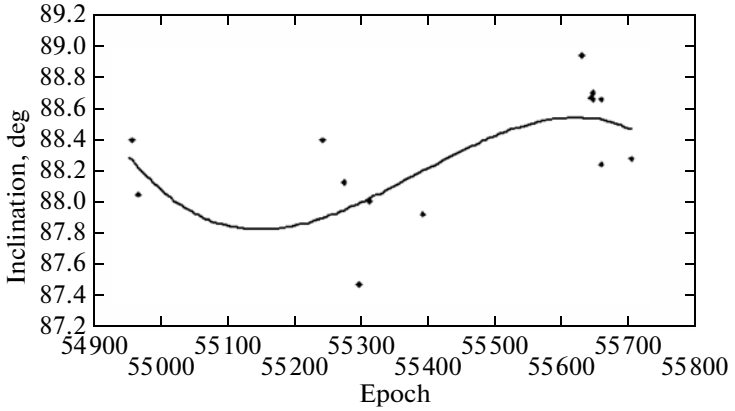

Fig. 8. Orbital inclination for HAT-P-12b versus time.

According to Bodenheimer et al. (2003), the equilibrium temperature of a planetary atmosphere can be defined as

$$T_{\rm eq} = T_{\rm eff}\left[\frac{R_{\rm S}}{2a(1+e^2/2)}\right](1-A)^{1/4}, \qquad (6)$$

where $T_{\rm eff}$ is the effective temperature and $R_{\rm s}$ is the stellar radius.

Table 4. Temperature and albedo estimates for the atmospheres of exoplanets

Exoplanet	Temperature of planetary atmosphere, $T_{\rm eq}$ (K)	Albedo of planetary atmosphere
GJ1214b	497	0.32
Qatar-1b	1270	0.30
WASP-10b	939	0.32
WASP-12b	2423	0.15
WASP-14b	1680	0.30
WASP-24b	1500	0.30
WASP-39b	1030	0.30
WASP-40b	1571	0.32
WASP-48b	1486	0.30
TrES-3b	1500	0.28
HAT-P-9b	1394	0.30
HAT-P-12b	854	0.32
HAT-P-18b	767	0.32
HAT-P-20b	880	0.32
Kepler-6b	780	0.32
HD209458b	1285	0.30
KOI 256b	1160	0.28
KOI 194b	1133	0.28
KOI 425b	967	0.13

Using relation (6) and the dependence $T_{\rm eq}(A)$ presented in Fig. 3 from Demory et al. (2011), we will determine the equilibrium temperature $T_{\rm eq}$ and, in the cases where $T_{\rm eq}$ has been determined previously, the albedo A. The results of our calculations are presented in Table 4.

CONCLUSIONS

Based on our observations performed with the automated Pulkovo Astronomical Observatory telescopes, we obtained transit light curves for 16 known exoplanets and six transit observations for three exoplanet candidates discovered by the Kepler Space Telescope. For the object KO I 256b, we detected a strong deviation of its orbital revolution from the theoretically predicted one. For the other exoplanet WASP-12b, we detected large variations of the transit light curve that could be caused by the planet transit across the parts of the stellar disk where spots were present or by the presence of a satellite around this planet. For the exoplanet HAT-P-12b, the periodic variations in transit duration found may be indicative of variations in its orbital inclination. We estimated the transit duration and depth, the central transit time, and the radius and orbital inclination of the planet. The characteristic equilibrium temperature and albedo of the planetary atmosphere were estimated for several exoplanets.

REFERENCES

1. E. Agol, J. H. Steffen, R. Sari, and W. Clarkson, Mon. Not. R. Astron. Soc. **359**, 567 (2005).
2. J. W. Barnes, arXiv: 0708.0243 (2007).
3. P. Bodenheimer, G. Laughlin, and D. N. C. Lin, Astrophys. J. **592**, 552 (2003).
4. W. J. Borucki and the KEPLER Team, arXiv:1102.0541v1 (2011).
5. C. J. Burke, arXiv: 0801.2579 (2008).

6. T. Chan, M. Ingemyr, J. N. Winn, et al., http://arxiv.org/abs/1103.3078 (2011).
7. W. Danchi, *2008 Exoplanet Forum Rep. 71,* Ed. by P. R. Lawsan, W. A. Traub, and S. C. Unwin (NASA JPL, Pasadena, CA, 2008).
8. B.-Q. Demory, S. Seager, N. Madhusudhan, et al., Astrophys. J. **735**, L12 (2011).
9. A. V. Devyatkin, I. I. Kanaev, A. P. Kulish, et al., Izv. GAO **217**, 505 (2004).
10. A. V. Devyatkin, A. P. Kulish, I. A. Vereshchagina, et al., J. Opt. Technol. **75**, 59 (2008).
11. A. V. Devyatkin, D. L. Gorshanov, V. V. Kupriyanov, et al., Solar Syst. Res. **43**, 229 (2009).
12. S. Hoyer, P. Rojo, M. Lopez-Morales, et al., Astrophys. J. **733**, 53 (2011).
13. I. I. Kanaev, A. V. Devyatkin, A. P. Kulish, et al., Izv. GAO **214**, 523 (2000).
14. A. P. Kulish, A. V. Devyatkin, V. B. Rafalskii, et al., Izv. GAO **219**, 192 (2009).
15. J. Miralda-Escude, Astrophys. J. **564**, 1019 (2002).
16. N. Narita, arXiv:0906.0769 (2009).
17. S. Poddany, L. Brat, and O. Pejcha, New Astron. **15**, 297 (2010).
18. V. L. Straizys, *Multicolor Stellar Photometry* (Mosklas, Vil'nyus, 1977; Pachart Publ., Tucson, 1992).
19. B. Tingley and P. D. Sackett, Astrophys. J. **627**, 1011 (2005).
20. V. V. Vityazev, *Wavelet Analysis of Time Series* (SPb. Gos. Univ., St.-Petersburg, 2001a) [in Russian].
21. V. V. Vityazev, *Time Series Analysis of Unequally Spaced Data* (SPb. Gos. Univ., St.-Petersburg, 2001b) [in Russian].

Translated by V. Astakhov